Crystallization in Oriented Semicrystalline Diblock Copolymers

Ian W. Hamley

School of Chemistry, University of Leeds, Leeds, W. Yorkshire LS2 9JT, U.K.

J. Patrick A. Fairclough, Nicholas J. Terrill, and Anthony J. Ryan*

Manchester Materials Science Centre, UMIST, Grosvenor Street, Manchester M1 7HS U.K.

Paul M. Lipic and Frank S. Bates

Department of Chemical Engineering and Materials Science, University of Minnesota, Minneapolis, Minnesota 55455

Elizabeth Towns-Andrews

CLRC Daresbury Laboratory, Warrington WA4 4AD, U.K.

Received March 4, 1996; Revised Manuscript Received October 10, 1996[⊗]

ABSTRACT: Crystallization in oriented diblock copolymers containing poly(ethylene) (PE) has been investigated using simultaneous small-angle and wide-angle X-ray scattering (SAXS/WAXS). The orientation of the crystallized PE stems was deduced from the orientation of peaks in the WAXS pattern with respect to those in the SAXS to be parallel to the lamellar interface for symmetric diblocks containing PE and either a rubbery or glassy amorphous block. For a symmetric diblock with a poly(vinylcyclohexane) block that is glassy at room temperature we observe diffuse scattering parallel to the meridian in the SAXS pattern that is consistent with lateral correlations between PE crystallites within the layers of semicrystalline PE. In contrast, in all the samples containing an amorphous component, PE crystallization occurred with no lateral positional correlations of crystallites. Crystallization in asymmetric diblocks with compositions $f_{PE} = 0.35$ and 0.46 was also investigated. It was found that a lamellar structure is the stable solid structure and that this melts epitaxially to a hexagonal-packed cylinder structure in the $f_{PE} = 0.35$ sample. For the $f_{PE} = 0.46$ sample that forms a perforated layer phase in the melt, chain-folded PE stems were found to be parallel to the lamellar interface, as for the symmetric diblocks.

1. Introduction

Crystallization is of fundamental importance to the ultimate properties and applications of many commercially important polymers. The crystal structures of many industrially important polymers such as poly(ethylene) and poly(propylene) have been extensively studied and reported upon. However, crystallization in more complex polymer architectures such as block copolymers has yet to be systematically studied.

In a block copolymer, chemically distinct polymer chains are linked at their ends. This enables the control of material properties, because under ambient conditions different blocks can be in the rubbery or amorphous state, the glassy state, or the crystalline state. By controlling the composition of the copolymer, quantified by the volume fractions of the components, it is thus possible to prepare structures such as particles of solidified polymer in a rubbery matrix. This ability to tailor material properties by modifying the molecular structure is a unique property of block copolymers.

In completely amorphous diblock copolymers, the polymer chains can be homogeneously mixed by increasing the temperature or decreasing the molecular weight.[1] As the temperature is lowered, the blocks tend to segregate to lower the free energy of mixing. The same effect can be achieved at fixed temperature by increasing the degree of polymerization. Segregated, or microphase-separated, block copolymers can form a variety of ordered structures below the order−disorder transition.[1] The lamellar, hexagonal-packed cylinder (hex.) and body-centered cubic micelle phases that are stable over a wide temperature range, depending on copolymer composition, are supplemented by a variety of complex phases that have recently been observed near the order−disorder transition (ODT). Hexagonal modulated lamellar (HML), hexagonal perforated layer (HPL), and $Ia\bar{3}d$ bicontinuous cubic structures have all been observed in the phase diagram between the lamellar and hexagonal-packed cylinder phase boundaries.[2]

In semicrystalline diblock copolymers that form ordered structures in the melt, the process of crystallization of one of the blocks is expected to compete with microphase separation at low temperatures. In fact, we have shown in a previous study of diblock copolymers containing an amorphous poly(1-ethylethylene) (PEE) or poly(1-methylbutane-1,4-diyl) (PEP)[3] block together with poly(ethylene) (PE) that crystallization completely overwhelms microphase separation[4] (structural diagrams of the polymers considered here are presented in Figure 1). A lamellar structure containing crystallites of chain-folded poly(ethylene) was formed as lamellar or hexagonal-packed cylinder melt structures were destroyed below the poly(ethylene) melting temperature, $T_m \sim 106$ °C. The change in domain spacing upon crystallization was studied using synchrotron small-angle X-ray scattering (SAXS). Simultaneous wide-angle X-ray scattering (WAXS) confirmed unambiguously the crystallization of PE in its usual orthorhombic form. The degree of crystallinity of the PE block determined from differential scanning calorimetry (DSC) measurements was found to be (40 ± 10)% for all PE−PEE samples with compositions $f_{PE} = 0.25$, $f_{PE} \simeq 0.5$, and $f_{PE} = 0.75$ that we studied. The kinetics of crystallization were investigated by computing the integrated SAXS invariant (which is a measure of the total small-angle scattering of the sample and hence is related to

* To whom correspondence should be addressed.

⊗ Abstract published in *Advance ACS Abstracts,* December 15, 1996.

S0024-9297(96)00343-9 CCC: $12.00

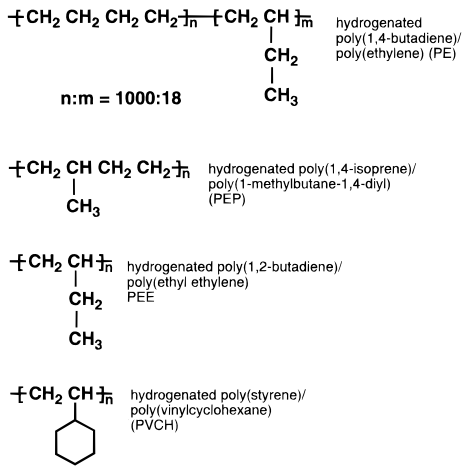

Figure 1. Structural diagrams for the components of the diblocks studied.

the density change on crystallization) as a function of time following a quench below T_m. The relative degree of crystallinity was shown to follow Avrami-type kinetics with an exponent $n = (3.0 \pm 0.1)$, consistent with a nucleation and growth process such as the formation of semicrystalline spherulites.[4]

Our previous work is complemented by the SAXS/WAXS and DSC studies of Rangarajan and co-workers.[5,6] They studied a range of PE−PEP diblock copolymers with PE volume fractions from $f_{PE} = 0.12$ to 0.56 forming a homogeneous phase in the melt. For all samples, crystallization in a lamellar structure occurred below T_m, and there was no indication of the formation of ordered structures in the melt.[5] In subsequent work,[6] the dynamics of crystallization in several PE−PEP and PE−PEE diblocks were studied and the development of up to four orders of SAXS peaks was found to be rapid and simultaneous following crystallization. During this process the location of the SAXS peaks was constant, suggesting a nucleation and growth process for the ordered structure.

Although Rangarajan and co-workers did not study oriented samples, they suggest a model for their samples crystallized from the homogeneous melt in which the PE domain consists of crystallites with chains folded perpendicular to the interface alternating with amorphous regions.[5] This is in contrast to the X-ray scattering results of Douzinas and Cohen on oriented PE−PEE diblocks crystallized from the heterogeneous melt.[7] By analyzing pole figures from WAXS data, they found that the crystallized PE chains are folded parallel to the lamellar interface that separates semicrystalline PE and amorphous PEE regions. On the other hand, a model with chains perpendicular to the interface was presented on the basis of SAXS/WAXS and electron microscopy data for crystallized poly(ethylene oxide)−poly(isoprene) (PEO−PI) diblocks.[8] A crystalline lamellar structure was observed when the PEO−PI samples were cast from ethyl benzene, which is a selective solvent for poly(isoprene) so that microphase separation does not precede crystallization. When cast from the nonselective solvent benzene, however, PEO crystallization was found to occur within microphase-separated morphologies. These morphologies may not be in equilibrium because the crystallizable block can precipitate from solution, causing the amorphous domains to adopt nonequilbrium structures.[9] WAXS data was also found to be consistent with perpendicular chain folding for low molecular weight poly(oxyethylene)−poly(oxybutylene) diblocks.[10]

In this work, we study the structure of a range of oriented diblock copolymers containing hydrogenated poly(1,4-butadiene) (PE) crystallized from the ordered melt using simultaneous SAXS/WAXS and transmission electron microscopy (TEM). The samples were oriented in the melt using shear and then rapidly quenched in liquid nitrogen prior to our synchrotron experiments. Solvent casting was not used to prepare crystallized samples, in an effort to minimize nonequilibrium morphologies. We compare crystallization in a sample which has a glassy component at room temperature (poly(vinylcyclohexane), PVCH, glass transition temperature $T_g \simeq 140$ °C) with the structure of crystallized samples containing PEE and PEP that are amorphous at room temperature ($T_g \simeq -20$ and -56 °C, respectively). The PE−PVCH sample is compositionally symmetric, forming a lamellar structure in the melt, and we compare the solid structure to symmetric PE−PEE and PE−PEP samples. In addition, we have investigated the influence (if any) of melt morphology on the crystallized structure by studying PE−PEE diblocks with hex. and HPL structures in the melt. The orientation of chain stems in PE crystallites is deduced by comparing the orientation of peaks in the SAXS and WAXS patterns.

2. Experimental Section

2.1. Sample Preparation. Full details of the acyclic polyolefin polymer synthesis and characterization are given elsewhere.[11] Here we merely summarize the general methods. The deuterated polyolefin diblocks were synthesized by catalytic deuteration of poly(diene) precursors, which in turn were anionically polymerized from butadiene and isoprene momomers (obtained from the Aldrich Chemical Co.). The precursor for poly(ethylene) is poly(1,4-butadiene), and that for poly(1-ethylethylene) is poly(1,2-butadiene), while that for poly(1-methylbutane-1,4-diyl) is poly(1,4-isoprene) (see Figure 1). Some samples were deuterated to provide contrast for neutron scattering experiments; however this does not change the X-ray scattering constrast relevant to our synchrotron experiments.

For the polyolefins containing PVCH a monodisperse poly(styrene)−poly(1,4-butadiene) diblock copolymer was anionically synthesized in cyclohexane using a lithium counterion. A two-step saturation process was completed using a homogeneous Wilkinson's catalyst, followed by a $Pd/BaSO_4$ heterogeneous catalyst to produce a poly(ethylene)−poly(vinyl cyclohexane) (PE−PVCH) diblock. A more detailed report discussing the two step saturation process has been given elsewhere.[12] This nearly symmetric sample is denoted PE−PVCH-1.

The block microstructures were characterized using ^1H NMR, as described elsewhere.[13] The number average molecular weights were determined from the synthesis stoichiometry, which we have found to be a reliable measure of the molecular weight. In addition, light scattering experiments were performed on selected polyolefin diblocks or diene precursors for PE−PEP and PE−PEE copolymers to determine weight-average molecular weights. Molecular weight polydispersities were determined using size exclusion chromatography (SEC) on the polyolefin diblock copolymers and diene diblock precursors. For all polymers the molecular weight distribution was narrow ($M_w/M_n < 1.1$). The volume fraction of PE, number average degree of polymerization, ODT, and assignments of melt morphology for all diblocks studied are presented in Table 1.

For the small-angle X-ray scattering (SAXS) studies monodomain samples of the copolymer were studied following shear, applied using a specially constructed oscillatory shear machine described elsewhere,[14] which operates with a simple

Table 1. Diblock Copolymers Studied

sample (b1−b2-no.)	f_1	10^{-3} M_n/kg mol^{-1}	T_{ODT}/°C (±2 °C)	ordered phases
PE−PVCH-1	0.52	15	238	lamellae
PE−PEE-21	0.35	81	>300	hex.
PE−PEE-20	0.46	81	>300	HPL
PE−PEE-22	0.50	81	>300	lamellae
PE−PEP-3	0.50	128	159	lamellae

shear geometry. Samples were sheared in the melt, quenched to room temperature, and then cut up in three orthogonal planes, defined by the shear direction, gradient, and vorticity, so that morphologies could be studied in different orientations with respect to the shear direction. In this paper we refer to parallel, perpendicular, and through orientations with respect to the shear direction in the layer plane.

2.2. Synchrotron X-ray Scattering. The synchrotron scattering experiments were performed on station 16.1 at the SRS, Daresbury Laboratory, Warrington, U.K. This is a fixed wavelength (1.41 Å), high-intensity diffraction station optimized for low-angle measurements.[15] Prior to monochromatization the incident beam is defined via a Kratky style aperture (positioned as close to the wiggler magnet tangent point as possible) and water-cooled horizontal and vertical apertures. The X-ray beam is monochromated and horizontally focused using a Ge(111) triangular crystal which is capable of accepting a 12 mrad horizontal aperture. The vertical focusing of the beam is achieved by bending a 1.2 m Pt-coated fused quartz mirror. Further beam definition is performed using post-monochromator vertical and horizontal slits. In this configuration, the predicted flux at the sample is $\sim 10^{13}$ photon/s. The SAXS data were either acquired using a two-dimensional multiwire gas detector with 512 × 512 pixels or a Molecular Dynamics phosphor imager. A vacuum chamber between the sample and the detector reduced air scattering and absorption. WAXS patterns were obtained using an image plate, through which a central hole was drilled to allow passage of the X-rays to the SAXS detector. Samples were attached to a sample holder using kapton tape, and heating was achieved using a resistive heater and a variac. The SAXS data were corrected for detector response (via uniform illumination with an ^{55}Fe source) and background scattering. The q ($=4\pi(\sin\theta)/\lambda$) scale was calculated using a sample of wet collagen (rat tail) for calibration.

2.3. Transmission Electron Microscopy. The morphology of selected PE−PEE diblocks was investigated using transmission electron microscopy. The TEM specimens were microtomed at −100 °C with a Reichert ultramicrotome fitted with a diamond knife. Slices were stained by exposure to RuO_4 vapors for 45 min. The rubbery amorphous block, i.e. PEE, is preferentially stained due to reduced diffusivity of RuO_4 in the other semicrystalline domain.[16] TEM images were obtained with a JEOL 1210 microscope operated at 120 keV. Prior to TEM experiments samples were shear oriented as follows: PE−PEE-21 was sheared at a rate $\omega = 0.01$ rad s^{-1} (100% strain amplitude) at 150 °C for 8 h and then annealed at 150 °C under vacuum for 87 h. PE−PEE-22 was subjected to the same shear treatment as PE−PEE-21 and then annealed at 150 °C under vacuum for 34 h sealed in a glass vial. PE−PEE-20 was sheared for 7.5 h at 150 °C ($\omega = 0.1$ rad s^{-1}, 100% amplitude) and then annealed for 673 h at 150 °C sealed in a glass vial.

3. Results and Discussion

3.1. Symmetric Diblocks. We first consider the PE−PVCH sample which contains a component that is glassy at room temperature. The SAXS and WAXS patterns obtained at room temperature are presented in Figure 2. In the perpendicular orientation, the SAXS pattern clearly shows two orders of reflection on the meridian (Figure 2a) and is consistent with the expected lamellar morphology for this sample. Also evident are two bands of diffuse scattering centered on $q_\perp = 0.044$ Å^{-1}. This diffuse scattering is evidence for lateral structure within the projection of the lamellar planes in this orientation. Detailed modeling of this structure (to be discussed) suggests that the PE lamellae contain a quasi-periodic one-dimensional lattice of crystallites. The WAXS data (Figure 2c) indicate oriented crystallites of PE. The inner diffuse ring of scattering arises from amorphous PVCH and PE, and superimposed on this are four (110) type reflections (at an angle $\phi \simeq 53°$ with respect to the vertical axis) and two meridional (200) type peaks. The angle ϕ is close to the value expected ($\phi = 56°$) for the diffraction pattern of the projection along the c axis of the body-centered orthorhombic PE unit cell.[17] The 2θ values of the peaks are close to those observed for the PE homopolymer, showing that the crystal structure is not substantially distorted when crystallization occurs between glassy walls in the solidified block copolymer. In this and all subsequent WAXS patterns for crystallized samples, the (110) reflections occur at $2\theta(\text{Cu K}_\alpha) = 21°$, and the outer (200) reflections at $2\theta(\text{Cu K}_\alpha) = 24°$.

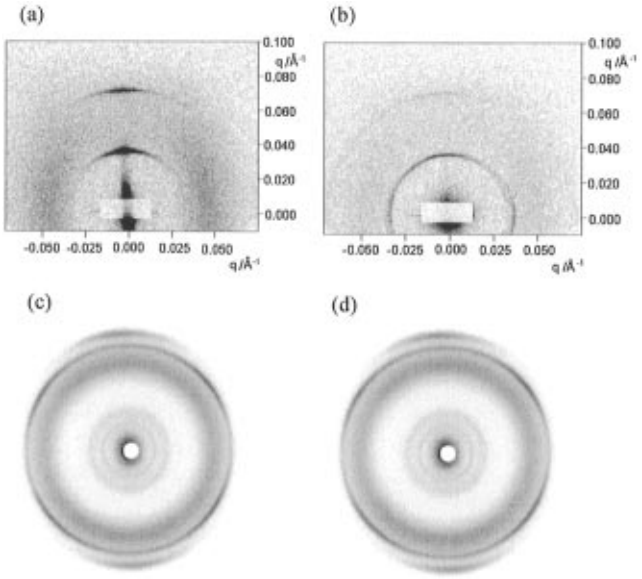

Figure 2. Scattering patterns obtained for PE−PVCH-1 at room temperature. (Top) SAXS patterns; (bottom) WAXS patterns; (left) perpendicular orientation; (right) parallel orientation.

For the parallel orientation, the SAXS data (Figure 2b) indicate that imperfect orientation was achieved, because the Bragg reflections are smeared into arcs. The diffuse scattering bars seen for the perpendicular orientation are also present, although weaker than for the former orientation. This indicates that the lateral correlations in the projection of the lamellar plane are weaker than for the perpendicular orientation. This can be understood because the lamellar alignment is poorer in the parallel orientation than in the perpendicular orientation, as a result of the shear process. The WAXS data (Figure 2d) are also consistent with the same orientation of the c axis in the PE unit cell as for the perpendicular orientation.

A dramatic change occurs when the sample is heated to 130 °C, i.e. above the PE melting temperature but below the PVCH T_g. Because the PVCH is still glassy, the orientation of the samples is retained. This is confirmed by the SAXS pattern for the perpendicular orientation in Figure 3a, where a peak oriented along the meridian is observed. An important observation is the absence of diffuse scattering bars parallel to the

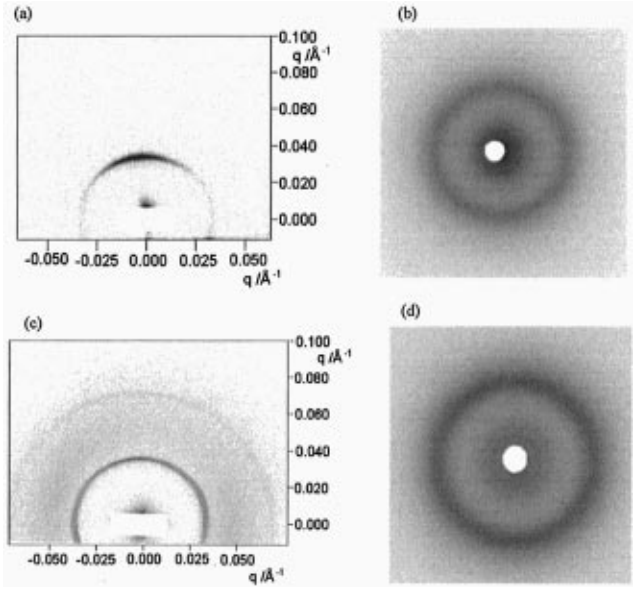

Figure 3. Scattering patterns obtained for PE−PVCH-1 at 130 °C: (Left) SAXS, (right) WAXS; (top) perpendicular orientation; (bottom) parallel orientation.

meridian. This is expected for molten PE and is consistent with our previous interpretation of this feature in terms of lateral correlations between PE crystallites. The WAXS pattern (Figure 3b) is similar to that observed for amorphous PE, because a diffuse ring at 2θ(Cu $K\alpha$) ≃18° is the only feature. In the SAXS pattern for the parallel orientation (Figure 3c), several orders of reflection are observed. These are smeared into arcs, as in the solid phase, with a bimodal population of lamellar orientations predominantly perpendicular to the meridian. The weaker, higher orders of reflection are more clearly visible than for the perpendicular orientation, because the pattern was accumulated for longer. The diffuse scattering bars have again disappeared, while the WAXS pattern contains the diffuse circle of scattering at an angle 2θ(Cu $K\alpha$) ≃18° characteristic of molten PE (note that the sample−detector distance was different for Figure 3b,d so that the rings do not appear to be in the same place).

Figure 4 shows sections through the SAXS data for the PE−PVCH sample in the perpendicular orientation. Vertical cuts show the sharp Bragg peak at $q_{\parallel} = 0.035$ Å^{-1} in the solid phase, whereas the lamellar ordering in the melt is much weaker and Bragg peaks are not evident on the same scale. The horizontal sections show very clearly a diffuse scattering peak centered at $q_{\perp} = 0.044$ Å^{-1} for the solid sample, which is not present in the melt.

Because the (200) reflections in the WAXS pattern lie along the same direction as the Bragg peaks in the SAXS pattern taken concurrently, we can deduce the orientation of the chain-folded PE stems with respect to the layer normal. Because the stems lie long the *c* axis of the unit cell,[16] they must lie parallel to the layers. A schematic of the lamellar structure in PE−PVCH-1, showing the crystallized stem orientation and in-plane correlations of crystallites, is presented in Figure 5.

The SAXS/WAXS patterns taken at room temperature for a symmetric polymer that contains a block that is amorphous at room temperature, PE−PEE-22, are presented in Figure 6. The SAXS data for the perpendicular and parallel orientations (Figure 6a,b) contain at least one sharp Bragg reflection (unfortunately the sample-detector distance was not optimal for this sample

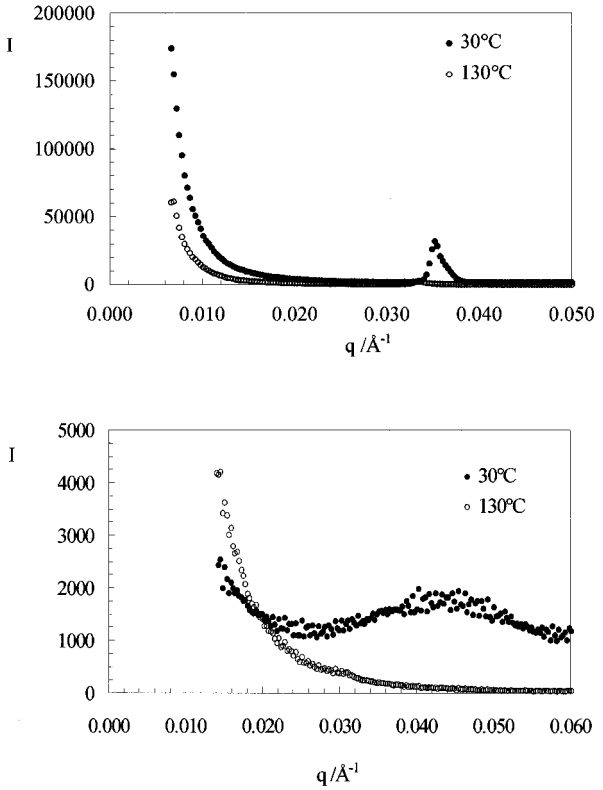

Figure 4. Sections through PE−PVCH-1 SAXS data. Key: Filled circles, solid; open circles, melt; (a) vertical, (b) horizontal.

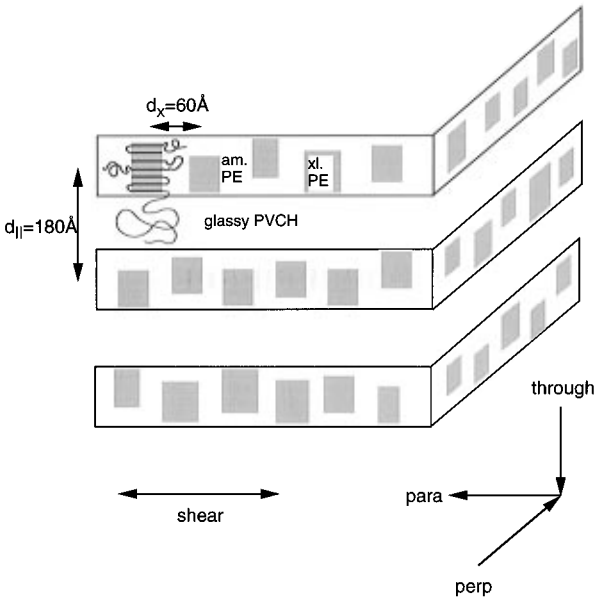

Figure 5. Qualitative model for the lamellar organization in the semicrystalline PE−PVCH sample. The PE domain consists of amorphous and crystalline regions, with a preferred intercrystallite separation as shown by the Markov model (Figure 17). The convention used to label the scattering patterns is also shown.

that has a large period d ≃710 Å and some reflections are obscured by the beam stop). The SAXS pattern for the through orientation (Figure 6c) shows a ring that is much lower in peak intensity than the Bragg peaks in the other two orientations. These data together are consistent with a lamellar structure, as expected for this symmetric diblock. This is confirmed by the representative TEM image shown in Figure 7 for this sample shear oriented and annealed at 150 °C, which shows

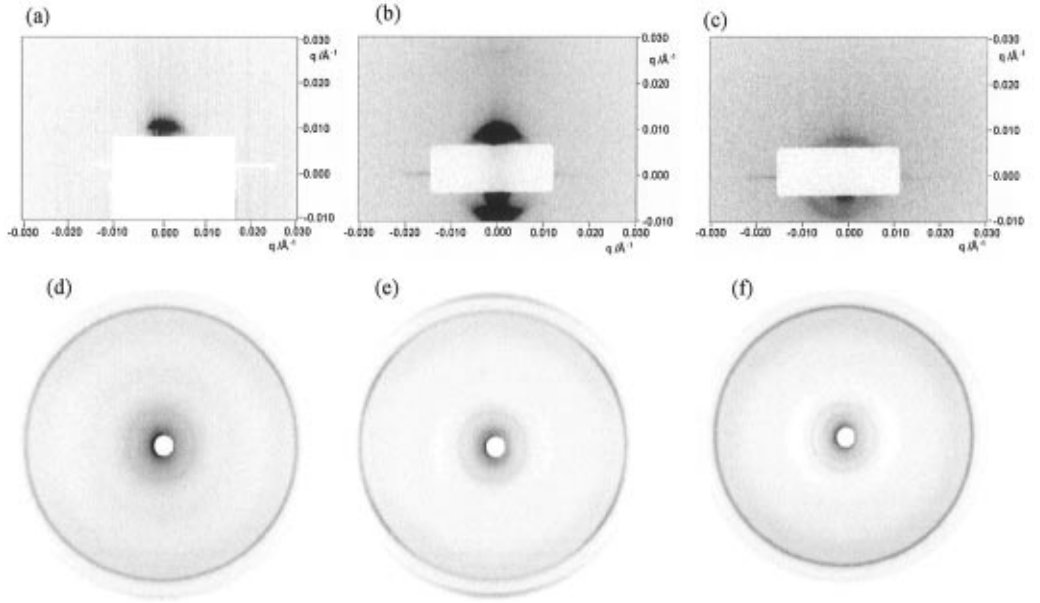

Figure 6. Scattering patterns obtained for PE−PEE-22D at room temperature: (Top) SAXS; (bottom) WAXS; (left) perpendicular; (center) parallel; (right) through.

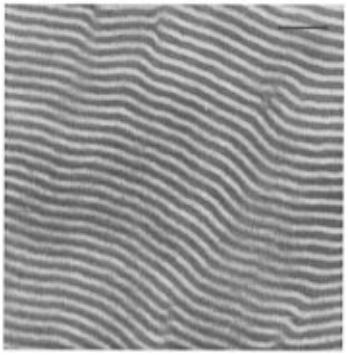

Figure 7. Transmission electron microscopy image of PE−PEE-22, preferentially stained with RuO_4. The scale bar represents 200 nm.

well-defined lamellae and characteristic edge dislocations. The WAXS pattern for the perpendicular and parallel orientations (Figure 6d,e) is similar to that observed for oriented semicrystalline PE. However, the orientation of the *c* axis of the unit cells within the lamellar planes is random, as shown by the isotropic scattering seen in the WAXS pattern for the through orientation (Figure 6f). The absence of diffuse scattering bars parallel to the meridian in the SAXS data indicates that there are no lateral correlations between the position of PE crystallites, in contrast to the PE−PVCH sample. However, isotropic diffuse scattering from amorphous PE is observed, as usual.[4]

We also performed X-ray scattering on a high molecular weight symmetric diblock containing an amorphous block, PEP. Representative SAXS/WAXS data for PE−PEP-3 at 30 °C are presented in Figure 8. The SAXS data for the perpendicular and parallel orientations show three integral orders of Bragg reflection, as expected for the lamellar morphology of this sample. The second-order reflection is weaker than the third, due to the form factor minimum that occurs for a diblock with $f = 0.5$. In contrast to the parallel and perpendicular orientations, there are no strong reflections in the SAXS pattern for the through orientation, again consistent with the lamellar structure of this sample. As for PE−PEE-22, the WAXS data indicate that the crystalline PE stems are oriented parallel to the layers in both the perpendicular and parallel orientations but not in the through orientation. There are no diffuse scattering bars in the SAXS data, which indicate that this sample behaves in this regard like PE−PEE-22 and unlike PE−PVCH-1.

Our observation of chain folding of semicrystalline PE stems parallel to the lamellae in these three symmetric diblocks is intriguing given that the PE stem must be normal to the lamellae at the PE−PEE interface. The general rules for obtaining a perpendicular orientation of chain stems with respect to the lamellar interface are that the polymers must be crystallizing from a disordered phase[6,10] or from a weakly segregated phase[6,18] and be of low molar mass. This is because there is a large length scale change from $d \sim N^{2/3}$ for a block copolymer melt to $d \sim N$ for a polymer with crystalline stems, where N is the degree of polymerization. As N increases or the polymer vitrifies, the interfacial area per block junction is increased and the stems then tilt[19] or eventually become parallel to the lamellae to match the interfacial areas of the two blocks, as shown in Figure 9. Crystallization can then occur without the free energy penalty that results from a change in domain spacing.

3.2. Asymmetric Diblocks. Changes in the SAXS pattern during a heat−cool cycle for PE−PEE-21, which has $f_{PE} = 0.35$ are shown in Figure 10. At 23 °C three orders of Bragg reflections are evident on the meridian, indicating a lamellar structure. Also clearly present is a ring of diffuse scattering from semicrystalline PE, centered at $q = 0.045$ Å^{-1}. In contrast to the lamellar structure found in the solid for this sample, the melt structure is hex. This is confirmed by the TEM image shown in Figure 11 which clearly shows a hexagonal-packed cylinder structure. Interestingly, the SAXS data for the melt show that the orientation of the microstructure has not been destroyed on melting, suggesting that the melt structure has developed from the solid, as illustrated in Figure 12.

The cross sections through the SAXS data shown in Figure 10d show that the location of the reflections at q^*, $\sqrt{4}q^*$, and $\sqrt{9}q^*$ do not change as the sample is

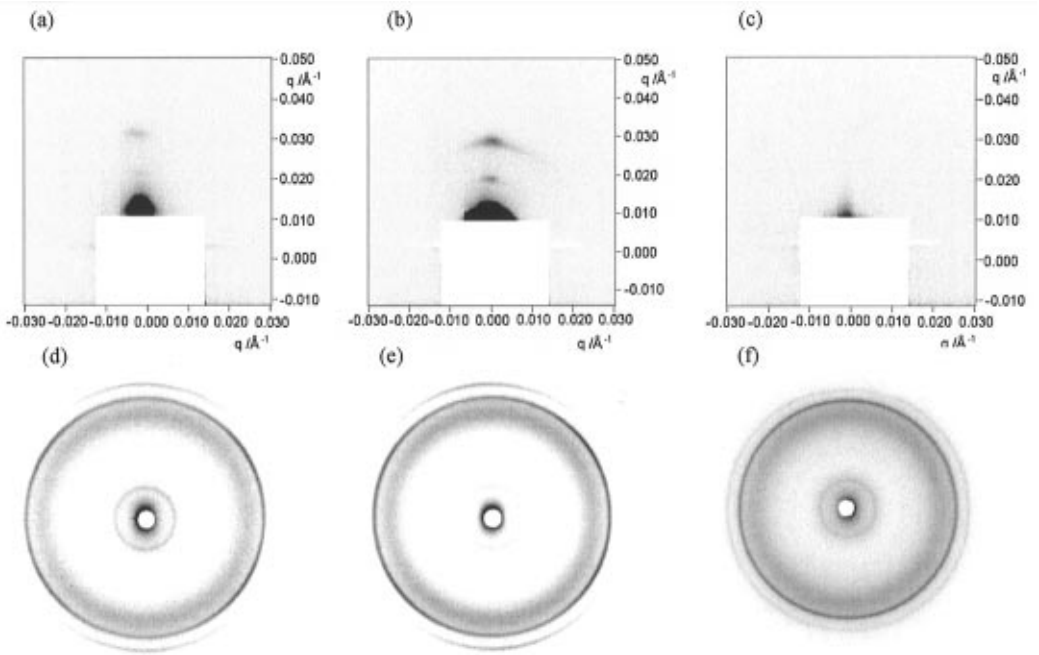

Figure 8. Scattering patterns obtained for PE−PEP-3H at room temperature: (Top) SAXS; (bottom) WAXS; (left) perpendicular; (center) parallel; (right) through.

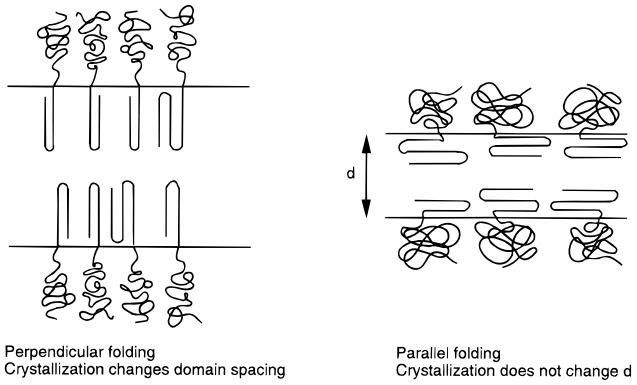

Figure 9. Illustration showing that the PE stem orientation upon chain folding in diblocks is controlled by the interfacial area per block junction.

heated from the solid into the melt. These reflections, together with the absence of the broad scattering peak from semicrystalline PE centered on $q = 0.045$ Å^{-1}, confirm that the sample has melted into an oriented hexagonal-packed cylinder structure. The $\sqrt{3}q^*$ and $\sqrt{7}q^*$ reflections expected in general for an unoriented hex. sample are missing from this pattern, because it corresponds to an oriented pattern from rods viewed edge-on. The fact that the sample orientation is maintained upon melting, together with the observation that the domain spacing does not change, suggests that melting from the lamellar phase to the hexagonal phase proceeds epitaxially. This epitaxial growth has also recently been observed for a poly(oxyethylene)−poly(oxybutylene) diblock with $f_{PEO} = 0.38$, heating from the solid phase where PEO is semicrystalline into a melt of hexagonal-packed cylinders.[20]

The WAXS patterns for the solid phase of this sample (not shown) are similar to those for unoriented semicrystalline PE, consisting of a sharp isotropic ring of (110) reflections superimposed on a diffuse scattering ring and a sharp isotropic (200) ring. Thus the crystallized PE stems are randomly oriented with respect to the lamellar planes in this asymmetric diblock, in contrast to the symmetric samples.

A representative TEM image for PE−PEE-20 shear oriented at 150 °C is shown in Figure 13. The presence of well-defined lamellae (noticeable in the corners of the picture) suggests a layered structure. In the central region of the picture the layers are broken up by perforations. TEM images with the beam normal to the shear plane show patches of hexagonal-packed holes, providing evidence that this sample forms a hexagonal perforated layer (HPL) phase (illustrated in Figure 14) in the melt. Even though it has a composition, $f_{PE} = 0.46$, close to symmetric, the shift of the phase boundaries caused by the large conformational asymmetry of the PE−PEE system[21] is sufficient to stabilize this structure. In the melt, the four integral orders of Bragg reflection observed for the perpendicular orientation (Figure 15) show that the structure is layered (the second order is found to be weak because the composition of the sample is close to $f = 0.5$). The signature of in-plane structure in the melt layered phase is the presence of the pronounced shoulder at $q \simeq 1.25q^*$ on the first-order peak, which we associate with the interperforation spacing.

The SAXS pattern for the perpendicular orientation of this sample at room temperature contains several orders of Bragg reflection along the meridian (Figure 16), and this is consistent with a layered structure in the solid. The orientation of the WAXS pattern with respect to the SAXS pattern is the same as for symmetric diblocks; thus, the chain-folded PE stems are again oriented in general parallel to the lamellar interface. The PE stem orientation in the crystallites is the same with respect to the lamellae, whether crystallization is from a simple layered structure or a hexagonal-perforated layer structure.

3.3. Model for the Diffuse Scattering. We have modeled the diffuse scattering bars in the SAXS pattern for PE−PVCH using a Markov model for a one-dimensional lattice.[22] This is equivalent to a one-dimensional Ising model with nearest-neighbor pair interactions.[23] Markov models have previously been

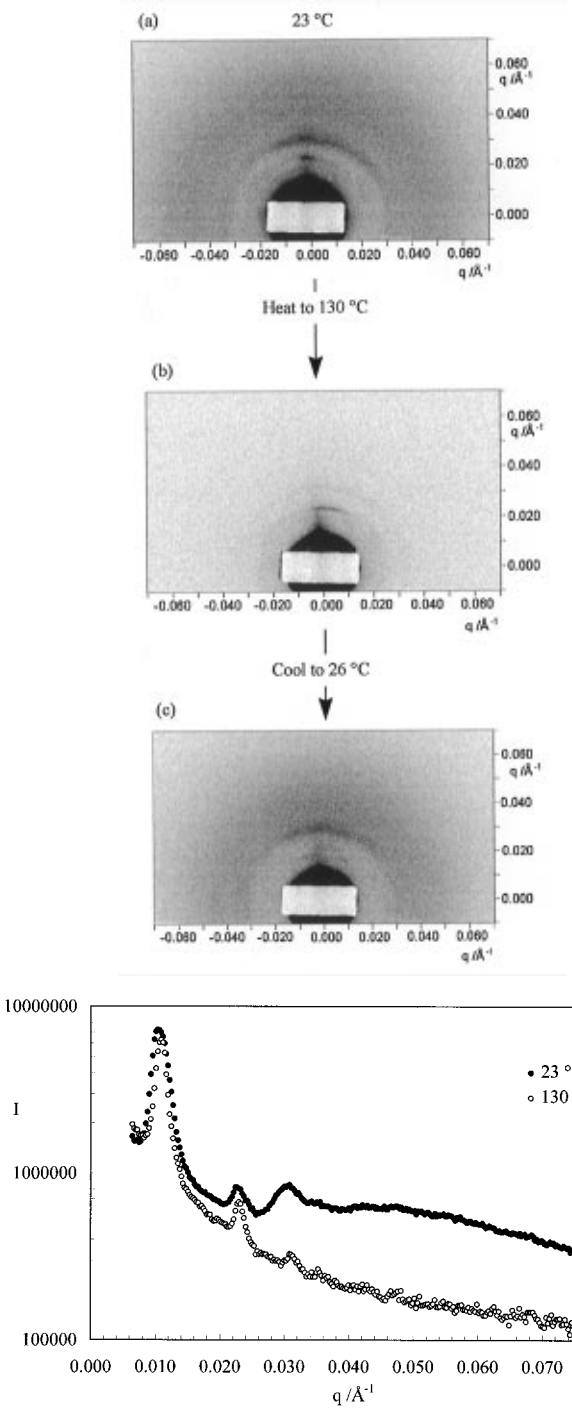

Figure 10. SAXS data for PE−PEE-21D during a heat−cool cycle: (a−c) SAXS patterns; (d) vertical sections through the data.

used to describe the kinetics of growth of lamellar crystals formed by chain-folding polymers,[24] but we are unaware of its application to describe diffuse scattering from semicrystalline polymers. In the Markov model, the probability of a site crystallizing ($A_{j,k} = 1$ if site crystalline, $A_{j,k} = 0$ otherwise) depends only on the occupancy of the previous site in that layer. In particular the probability for crystallite occupancy at site j in row k is given by

$$P(A_{j,k} = 1/A_{j-1,k}) = \alpha + \beta A_{j-1,k} \qquad (1)$$

Here α is the probability that a site is crystalline given that the preceding one is not, and β is the probability that a site is crystalline if the preceding one is also. A model with $\alpha = 0.8$ and $\beta = -0.6$ best describes our data in terms of the width of the diffuse scattering bars, and the overall fraction of sites occupied by crystallites is $\phi = 0.5$, close to the determined degree of crystallinity. An example of a stack of one-dimensional Markov lattices generated using this model is shown in Figure 17. On the basis of the location of the diffuse scattering bars with respect to the Bragg reflections observed for PE−PVCH-1, we use an in-plane repeat $d_x = 0.35\ d_{||}$, where $d_{||}$ is the layer period. Using a version of this model with a larger lattice size (300 × 300) than that shown in Figure 17, the scattered intensity is computed

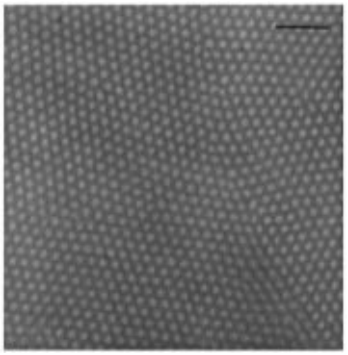

Figure 11. Transmission electron microscopy image of PE−PEE-21, preferentially stained with RuO_4. The scale bar represents 200 nm.

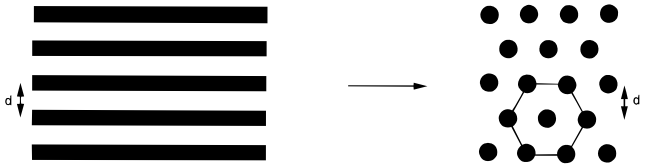

Figure 12. Epitaxial growth of a hexagonal-packed cylinder melt structure from a lamellar solid structure. The X-rays are incident in the direction of the arrow.

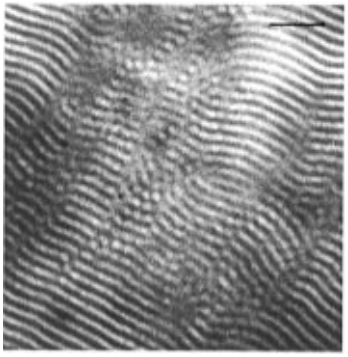

Figure 13. Transmission electron microscopy image of PE−PEE-20, preferentially stained with RuO_4. The scale bar represents 200 nm.

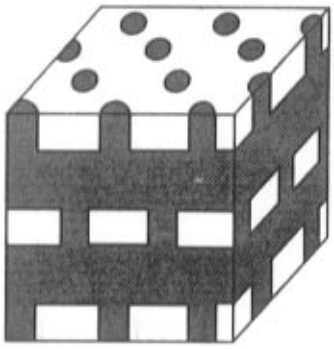

Figure 14. Structure of the HPL phase.

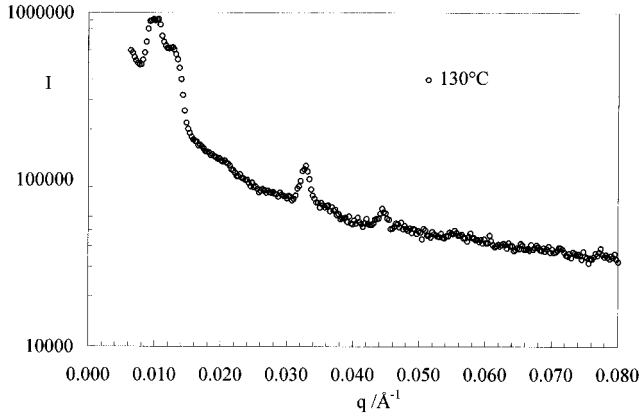

Figure 15. Vertical section through the SAXS from PE−PEE-20 in the perpendicular orientation at 130 °C.

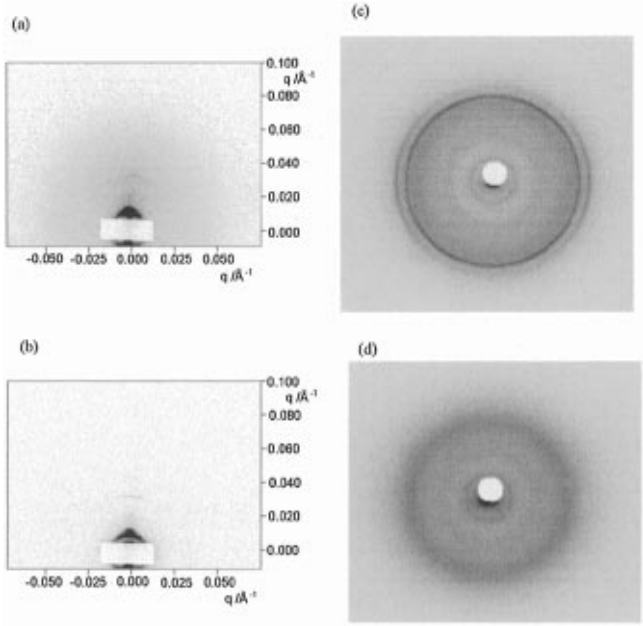

Figure 16. Scattering patterns from PE−PEE-20 in the perpendicular orientation: (Left) SAXS; (right) WAXS; (top) 23 °C; (bottom) 130 °C.

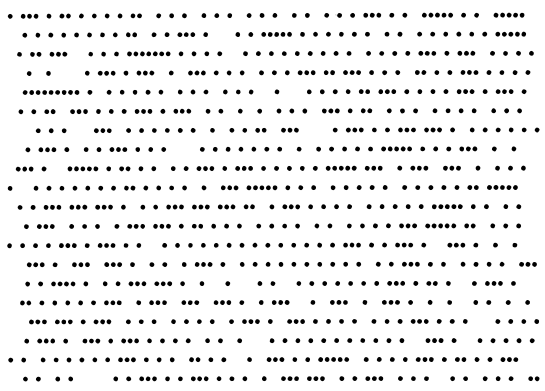

Figure 17. Realization of the lattice (with 20 × 80 points) used to model the SAXS pattern of PE−PVCH-1. The disorder within and between stacks of linear arrangements of crystallites (represented as points) leads to diffuse scattering.

as

$$I(q_x,q_y) = \sum_{j=1}^{N}\sum_{k=1}^{N}\sum_{l=1}^{N}\sum_{m=1}^{N} A_{j,k}A_{l,m} \exp[i(q_x X_{jl} + q_y Y_{km}] \quad (2)$$

Here $X_{jl} = x_j - x_l$ and $Y_{km} = y_k - y_m$, with $x_j = jd_x$, etc.,

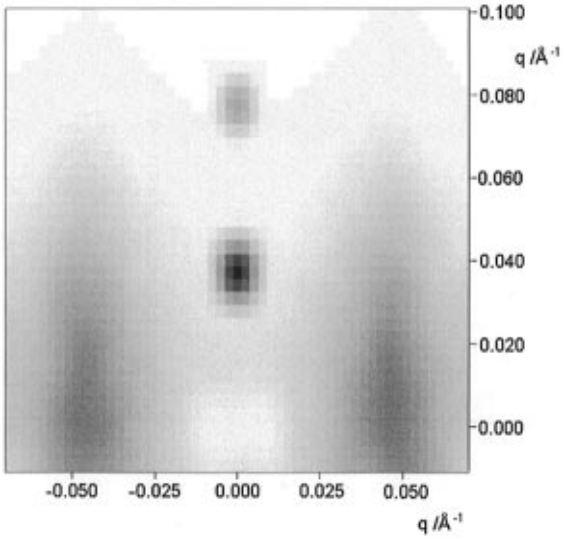

Figure 18. Scattering pattern computed for the model based on stacked Markov chains using $d_{||} = 180$ Å and $d_x = 0.35d_{||}$.

define intersite vectors. The calculated scattering pattern (Figure 18) may be compared to the SAXS data for the PE−PVCH sample in the perpendicular orientation (Figure 2a). The intensity is reduced at large q in the model due to the inclusion of a Debye−Waller factor, $\exp[-\sigma^2 q_x^2]$ with $\sigma^2 = 0.015$, that accounts for lattice disorder. Because we are not able to calculate a crystallite form factor, the Debye−Waller factor also simulates the effect of the reduction in intensity due to the form factor. The main features of the SAXS pattern are clearly reproduced in the model, especially the location and width of the diffuse scattering bar. However, the model does not account quantitatively for the relative intensities of the Bragg peaks and diffuse scattering, because it does not allow for the form factor of the crystallites. The diffuse scattering intensity from a one-dimensional Markov lattice is given by[22]

$$I(q)_{\text{diffuse}} = K(1 - \beta^2)[1 + \beta^2 - 2\beta \cos(qd_x)]^{-1}$$

where K is a constant. We anticipate this form for a cross section normal to the diffuse scattering bars in our model, because it consists of a stack of one-dimensional Markov lattices with no interlayer correlations. This model indeed fits a cross section through the diffuse scattering in the SAXS data for PE−PVCH-1 with $\beta = -0.64$ determined in a least-squares fit.

4. Summary

In summary, we have determined how poly(ethylene) crystallizes in nanoscale confinement by performing X-ray scattering experiments on shear-oriented diblock copolymers containing PE and either a rubbery or glassy amorphous block. For symmetric diblocks that form lamellar structures in the melt, PE crystallizes in a lamellar solid structure.

For symmetric and nearly symmetric diblocks (including the f_{PE} sample that forms a HPL phase in the melt), a comparison of the location of SAXS peaks from lamellae and WAXS peaks from the crystal unit cell shows that the poly(ethylene) chain folds with stems parallel to the lamellae for our samples which form lamellar phases in the melt. This is because the interfacial area per block junction is sufficiently large for glassy or amorphous blocks of high molecular weight to allow the PE stem to fold in this orientation. This

then allows crystallization to take place without an overall change in length scale. In a sample containing glassy PVCH, the crystallite positions are laterally correlated in the plane of the lamellae, as shown by meridional diffuse scattering bars in the corresponding SAXS patterns. A simple lattice model was shown to describe well the position and width of this diffuse scattering. For samples containing amorphous PEE or PEP on the other hand, poly(ethylene) crystallization occurred with no lateral positional correlations.

On the basis of the fixed position and orientation of SAXS peaks, an epitaxial relationship was observed on heating an $f_{PE} = 0.35$ sample from a lamellar solid phase into a hex. phase in the melt. The fact that this effect has also been observed for an $f_{PEO} = 0.38$ sample suggests that it may be a general mechanism for the growth of a hexagonal-packed cylinder melt phase from a semicrystalline lamellar solid.

Consistent with our previous results on unoriented asymmetric diblocks containing PE,[4] SAXS provides evidence for lamellar structures for the oriented semicrystalline samples studied here. However, in contrast to the symmetric and nearly symmetric samples, the PE unit cell in the asymmetric samples is not oriented with respect to the lamellar planes, as shown by the unoriented WAXS patterns.

Acknowledgment. A.J.R., I.W.H., and J.P.A.F. are grateful to the Engineering and Physical Sciences Research Council (U.K.) for the award of a research grant. Beamtime at Daresbury was provided by the EPSRC through the materials SESS. F.S.B. was supported by the U.S. National Science Foundation (Grant No. DMR 94-05101).

References and Notes

(1) Bates, F. S.; Fredrickson, G. H. *Annu. Rev. Phys. Chem.* **1990**, *41*, 525.
(2) Bates, F. S.; Schulz, M. F.; Khandpur, A. K.; Förster, S.; Rosedale, J. H.; Almdal, K.; Mortensen, K. *Faraday Discuss.* **1994**, *98*, 7.
(3) The structure-based name for this polymer is poly(1-methylbutane-1,4-diyl). The source-based name is hydrogenated poly(1,4-isoprene) (V. Metanomski, personal communication). It has previously been termed poly(ethylene−propylene) in numerous publications from the Bates and Fetters groups, and we use the abbreviation PEP for consistency with these earlier papers.
(4) Ryan, A. J.; Hamley, I. W.; Bras, W.; Bates, F. S. *Macromolecules* **1995**, *28*, 3860.
(5) Rangarajan, R.; Register, R. A.; Fetters, L. J. *Macromolecules* **1993**, *26*, 4640.
(6) Rangarajan, R.; Register, R. A.; Adamson, D. H.; Fetters, L. J.; Bras, W.; Naylor, S.; Ryan, A. J. *Macromolecules* **1995**, *28*, 1422.
(7) Douzinas, K. C.; Cohen, R. E. *Macromolecules* **1992**, *25*, 5030.
(8) Hirata, E.; Ijitsu, T.; Soen, T.; Hashimoto, T.; Kawai, H. *Polymer* **1975**, *16*, 249.
(9) Veith, C. A.; Cohen, R. E.; Argon, A. S. *Polymer* **1991**, *32*, 1545.
(10) Yang, Y.-W.; Tanodekaew, S.; Mai, S.-M.; Booth, C.; Ryan, A. J.; Bras, W.; Viras, K. *Macromolecules* **1995**, *28*, 6029.
(11) Rosedale, J. H.; Bates, F. S.; Almdal, K.; Mortensen, K.; Wignall, G. D. *Macromolecules* **1995**, *28*, 1429.
(12) Gehlsen, M. D.; Bates, F. S. *Macromolecules* **1993**, *26*, 4122.
(13) Bates, F. S.; Rosedale, J. H.; Bair, H. E.; Russell, T. P. *Macromolecules* **1989**, *22*, 2557.
(14) Koppi, K. A.; Tirrell, M.; Bates ,F. S.; Almdal, K.; Mortensen, K. *J. Rheology* **1994**, *38*, 999.
(15) Bliss, N.; Bordas, J.; Fell, B. D.; Harris, N. W.; Helsby, W. I.; Mant, G. R.; Smith, W. R.; Towns-Andrews, E. *Rev. Sci. Instrum.* **1995**, *66*, 1311.
(16) Khandpur, A. K.; Macosko, C. W.; Bates, F. S. *J. Polym. Sci. B* **1995**, *33*, 247.
(17) *Polymer Handbook*; Brandrup, J., Immergut, E. H., Eds.; Wiley: New York, 1989.
(18) Nojima, S.; Kato, K.; Yamamoto, S.; Ashida, T. *Macromolecules* **1992**, *25*, 2237.
(19) Craven, J. R.; Zhang, H.; Booth, C. *J. Chem. Soc., Faraday Trans.* **1994**, *87*, 1183.
(20) Ryan, A. J.; Fairclough, J. P. A.; Hamley, I. W.; Mai, S. M.; Booth, C. Manuscript in preparation.
(21) Hamley, I. W.; Gehlsen, M. D.; Khandpur, A. K.; Koppi, K. A.; Rosedale, J. H.; Schulz, M. F.; Bates, F. S.; Almdal, K.; Mortensen, K. *J. Phys. Fr.*2 **1994**, *4*, 2161.
(22) Welberry, T. R. *Rep. Prog. Phys.* **1985**, *48*, 1543.
(23) Enting, I. G. *J. Phys. C* **1977**, *10*, 1379.
(24) Gates, D. J.; Westcott, M. *Proc. R. Soc. London A* **1988**, *416*, 443.

MA960343A